

Gluon fragmentation functions in the Nambu-Jona-Lasinio model

Dong-Jing Yang*

*Department of Physics, National Taiwan Normal University,
Taipei 10610, Taiwan, Republic of China*

Hsiang-nan Li†

*Institute of Physics, Academia Sinica,
Taipei 11529, Taiwan, Republic of China*

(Dated: July 20, 2016)

Abstract

We derive gluon fragmentation functions in the Nambu-Jona-Lasinio (NJL) model by treating a gluon as a pair of color lines formed by fictitious quark and anti-quark ($q\bar{q}$). Gluon elementary fragmentation functions are obtained from the quark and anti-quark elementary fragmentation functions for emitting specific mesons in the NJL model under the requirement that the $q\bar{q}$ pair maintains in the flavor-singlet state after meson emissions. An integral equation, which iterates the gluon elementary fragmentation functions to all orders, is then solved to yield the gluon fragmentation functions at a model scale. It is observed that these solutions are stable with respect to variation of relevant model parameters, especially after QCD evolution to a higher scale is implemented. We show that the inclusion of the gluon fragmentation functions into the theoretical predictions from only the quark fragmentation functions greatly improves the agreement with the SLD data for the pion and kaon productions in e^+e^- annihilation. Our proposal provides a plausible construct for the gluon fragmentation functions, which are supposed to be null in the NJL model.

PACS numbers: 12.39.Ki, 13.60.Le, 13.66.Bc

*Electronic address: djyang@std.ntnu.edu.tw

†Electronic address: hnli@phys.sinica.edu.tw

I. INTRODUCTION

A fragmentation function contains important information on the strong dynamics of producing a hadron in high-energy scattering process. It describes the probability of a parton to emit mesons with certain fractions of the parent parton momentum, and serves as a crucial input to a framework for hadron production based on factorization theorem. For example, one needs unpolarized fragmentation functions for the analysis of semi-inclusive deeply inelastic scattering, electron-positron annihilation into hadrons, and hadron hadroproduction [1–11]. Quark fragmentation functions in the low energy limit have been calculated in effective models recently, such as the Nambu-Jona-Lasinio (NJL) model [12] and the nonlocal chiral quark model [13]. A concern is that gluon fragmentation functions are assumed to be null at a model scale, due to the absence of gluonic degrees of freedom in the corresponding Lagrangians. A gluon can certainly fragment into hadrons at a low scale, just like a quark does. Without the gluon fragmentation functions at a model scale, QCD evolution effects cannot be complete, and the resultant quark fragmentation functions at a high scale are not reliable. A simple argument is as follows. The quark fragmentation function $D_q^h(z)$ of a hadron h with a momentum fraction z obeys the sum rule $\sum_h \int z D_q^h(z) dz = 1$ for 100% quark light-cone momentum transfer to hadrons at a model scale. Setting the gluon fragmentation function $D_g^h(z)$ to zero will violate the sum rule $\sum_h \int z D_g^h(z) dz = 1$, so the quark and gluon fragmentation functions invalidate the sum rules after QCD evolution.

In this paper we attempt to derive the gluon fragmentation functions in the NJL model. Though there are lack of gluonic degrees of freedom, we regard a gluon as a pair of color lines formed by fictitious quark and anti-quark ($q\bar{q}$) in a color-octet state. A requirement is that the $q\bar{q}$ pair remains flavor-singlet after meson emissions. Namely, the quark q emits a hadron $m = q\bar{Q}$ and the anti-quark \bar{q} emits an anti-hadron $\bar{m} = Q\bar{q}$ at the same time, resulting in a flavor-singlet fictitious $Q\bar{Q}$ pair. The idea originates from the color dipole model, in which a gluon is treated as a pair of color lines, and parton emissions are turned into emissions of color dipoles composed of quarks and anti-quarks. The simplest version of our proposal leads to the formulation of the gluon fragmentation functions in terms of the quark fragmentation functions, similar to that in the Lund model [14]. A refined version is to include the mechanism of quark annihilation, which respects the flavor-singlet requirement on the $q\bar{q}$ pair, such that the specific flavor of the fictitious quarks is irrelevant. Gluon

elementary fragmentation functions in the refined version are constructed from the quark and anti-quark elementary fragmentation functions for emitting specific mesons in one step. An integral equation, which iterates the gluon elementary fragmentation functions to all orders, is then solved to yield the gluon fragmentation functions.

It will be verified that our results are stable with respect to variation of relevant model parameters, including the model scales and the fictitious quark masses, especially after QCD evolution to a higher scale is implemented. The possible effect from branching of a gluon into more, i.e., from the multi-dipole contribution, is also investigated, and found to be minor. With the gluon and quark fragmentation functions obtained in this paper, we predict the $e^+ + e^- \rightarrow h + X$ differential cross section at the scale $Q^2 = M_Z^2$, M_Z being the Z boson mass, and compare it with the measured ones, such as those from TASSO [15–17], TPC [18], HRS [19], TOPAZ [20], SLD [21], ALEPH [22], OPAL [23], and DELPHI [24, 25]. Since the above data are similar, we will focus on the SLD one. It will be demonstrated, as an appropriate model scale is chosen, that the inclusion of the gluon fragmentation functions into the predictions from only the quark fragmentation functions greatly improves the agreement with the SLD data for the pion and kaon productions. This work explores the behavior of the gluon fragmentation functions at low energy, and their importance on phenomenological applications.

The rest of the paper is organized as follows. We review the evaluation of the quark fragmentation functions in the NJL model in Sec. II. The color dipole model is briefly introduced in Sec. III, which motivates our proposal to treat a gluon as a pair of color lines. The gluon fragmentation functions are then formulated in the simple version, which is consistent with the Lund model, and in the refined version, which includes the quark annihilation mechanism and the multi-dipole contribution. Numerical results of the gluon fragmentation functions for the pion and kaon, before and after the next-to-leading-order (NLO) QCD evolution, are presented. These results are compared to the Hirai-Kumano-Nagai-Sudoh (HKNS) [26] and de Florian-Sassot-Stratmann (DSS) [27] parameterizations of the quark and gluon fragmentation functions in Sec. IV, and then to the SLD data of the $e^+ + e^- \rightarrow h + X$ differential cross sections at $Q^2 = M_Z^2$. Section V contains the conclusion. Some numerical results from the leading-order (LO) QCD evolution are collected in the Appendix for reference.

II. QUARK FRAGMENTATION FUNCTIONS

The NJL model [28, 29] is a low-energy effective theory, like the BCS theory, to demonstrate the chiral symmetry breaking and appearance of Nambu-Goldstone bosons. A non-vanishing chiral condensate would be generated as the coupling of the four-fermion interaction is greater than a critical value. The spontaneous chiral symmetry breaking then gives rise to dynamical quark mass from a gap equation. The spontaneous chiral symmetry breaking also induces massless Nambu-Goldstone bosons, represented by the pole of the summation of fermion loops to all orders in the four-fermion coupling, and regarded as quark-antiquark excitations of the spontaneously broken vacuum. To get massive Nambu-Goldstone bosons, one adds a bare fermion mass term, i.e., explicit chiral symmetry breaking, into the effective theory. The NJL model has been applied to the calculation of quark distribution functions [30, 31] and fragmentation functions [12] for massive pseudoscalar mesons.

In this section we briefly review the derivation of quark fragmentation functions for pseudoscalar mesons in the NJL model, which starts with the construction of an elementary fragmentation function $d_q^m(z)$. This function represents the probability of a quark q to emit a meson m in one step, which carries a light-cone momentum fraction z of the quark momentum in the minus direction, as depicted in Fig. 1. In the light-cone frame the quark possesses vanishing transverse momentum before the emission, and nonzero $k_T = -p_\perp/z$ with respect to the direction of the emitted meson. The elementary quark fragmentation function has been computed as [32]

$$\begin{aligned} d_q^m(z) &= -\frac{C_q^m}{2} g_{mqQ}^2 \frac{z}{2} \int \frac{d^4 k}{(2\pi)^4} \text{tr} [S_1(k) \gamma^+ S_1(k) \gamma_5 (\not{k} - \not{p} + M_2) \gamma_5] \\ &\quad \times \delta(k_- - p_-/z) 2\pi \delta((k - p)^2 - M_2^2) \\ &= \frac{C_q^m}{2} g_{mqQ}^2 \frac{z}{2} \int \frac{d^2 p_\perp}{(2\pi)^3} \frac{p_\perp^2 + [(z-1)M_1 - M_2]^2}{[p_\perp^2 + z(z-1)M_1^2 + zM_2^2 + (1-z)m_m^2]^2}, \end{aligned} \quad (1)$$

where C_q^m is a flavor factor, S_1 denotes the quark propagator, M_1 and M_2 are the quark constituent masses before and after the emission, respectively, and m_m is the meson mass. The dipole regulator in [33] has been employed to avoid a divergence in the above integral.

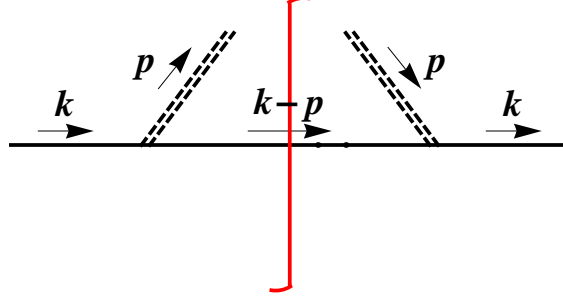


FIG. 1: Quark elementary fragmentation function for a pseudoscalar meson, in which the solid and dashed lines represent the quark and the pseudoscalar meson, respectively.

The quark-meson coupling g_{mqQ} is determined via the quark-bubble graph [32, 33]:

$$\frac{1}{g_{mqQ}^2} = -\frac{\partial \Pi(p)}{\partial p^2} \Big|_{p^2=m_m^2}, \quad (2)$$

$$\Pi(p) = 2N_c i \int \frac{d^4 k}{(2\pi)^4} \text{tr} [\gamma_5 S_1(k) \gamma_5 S_1(k-p)],$$

with the number of colors N_c .

We adopt the values $g_{\pi qQ} = 4.24$ and $g_{KqQ} = 4.52$ for the couplings, $M_u = M_d = 0.4$ GeV and $M_s = 0.59$ GeV for the quark constituent masses, and $m_\pi = 0.14$ GeV and $m_K = 0.495$ GeV for the meson masses. The curves of $z d_q^m(z)$ displayed in Fig. 2 indicate that the probability for emitting a meson with a vanishing momentum is tiny, and the meson which can be directly formed from the quark q in one step, such as the $u \rightarrow \pi^+$ and $s \rightarrow K^-$ channels, prefers a momentum fraction as high as $z \sim 0.7-0.8$. Since a kaon is more massive than a pion, it tends to carry a bit larger momentum fraction z . These features will help understanding our numerical results for the gluon fragmentation functions to be evaluated in the next section.

The integral equation based on a multiplicative ansatz for a fragmentation function is written as [34]

$$D_q^m(z) = \hat{d}_q^m(z) + \sum_Q \int_z^1 \frac{dy}{y} \hat{d}_q^Q(y) D_Q^m\left(\frac{z}{y}\right), \quad (3)$$

$$\hat{d}_q^Q(y) = \hat{d}_q^m(1-y)|_{m=q\bar{Q}},$$

where the elementary fragmentation function has been normalized into $\hat{d}_q^m(z)$ in order to have the meaning of probability. Equation (3), which iterates Eq. (1) to all orders, determines the probability of emitting a meson m by the quark q with a momentum fraction z through a jet

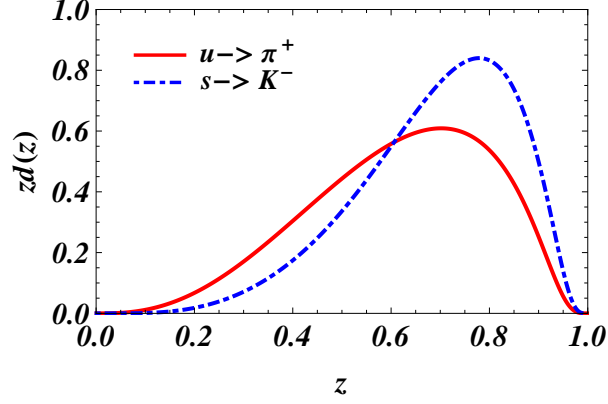


FIG. 2: z dependence of $z d_u^{\pi^+}(z)$ and $z d_s^{K^-}(z)$.

process: the first term \hat{d}_q^m on the right-hand side of Eq. (3) corresponds to the first emission of the meson $m = q\bar{Q}$ in the jet process, and the second term, containing a convolution, collects the contribution from the rest of meson emissions in the jet process described by D_Q^m with the probability \hat{d}_q^Q .

Equation (3) can be solved in at least three different ways to get the quark fragmentation functions, by iteration, by inverse matrix inversion, and by Monte Carlo simulation. Here we take the former two methods, and have confirmed that the results are the same. The z dependence of $z D_q^m(z)$ for $q = u, s$ and $m = \pi^\pm, K^\pm$ at a model scale is exhibited in Fig. 3. It is found that the quark fragmentation functions will have peaks in the high z region, if the mesons can be formed directly from the quarks (referred to the discussion on Fig. 2), such as the $u \rightarrow \pi^+, K^+$ and $s \rightarrow K^-$ channels. Otherwise, the mesons come from the secondary emissions, and the corresponding fragmentation functions are larger at low z . It is expected that the $u \rightarrow K^+$ channel has a smaller probability than the $u \rightarrow \pi^+$ one does, because a kaon is more massive. The same explanation applies to the comparison of the $u \rightarrow K^-$ ($s \rightarrow K^+$) and $u \rightarrow \pi^-$ ($s \rightarrow \pi^\pm$) channels.

III. GLUON FRAGMENTATION FUNCTIONS

Due to the absence of the gluonic degrees of freedom at the Lagrangian level in the NJL model, a gluon fragmentation function cannot be computed directly. As stated in the Introduction, we propose to derive this fragmentation function by treating a gluon as a pair of color lines formed by fictitious quark and anti-quark ($q\bar{q}$) in a color-octet state. The idea

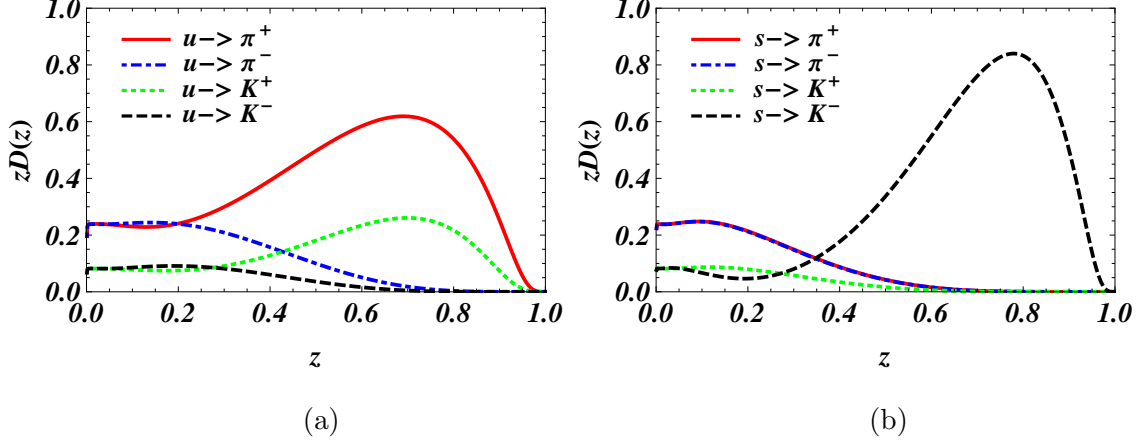


FIG. 3: z dependence of (a) $zD_u^m(z)$ and (b) $zD_s^m(z)$ from the NJL model at a model scale for $m = \pi^\pm$ and K^\pm .

originates from the color dipole model developed by Gustafson and Andersson in 80's [35–37]. The large N_c limit is assumed in this model, under which parton emissions are turned into emissions of color dipoles composed of quarks and anti-quarks in, for instance, a shower process. The color dipole model has been also extended to handle onium-onium scattering at high energy [14, 38], for which a high energy onium state, consisting of numerous $q\bar{q}$ pairs and soft gluons, is regarded as a collection of color dipoles in the large N_c limit. The result has been compared with that from the formalism with Balitskii-Fadin-Kuraev-Lipatov pomerons [38].

A requirement is that the fictitious $q\bar{q}$ pair remains flavor-singlet after meson emissions, which can be achieved by the simultaneous emissions of $m = q\bar{Q}$ and $\bar{m} = Q\bar{q}$ as illustrated in Fig. 4. That is, if the u quark of the $u\bar{u}$ pair fragments a π^+ meson, the \bar{u} quark of the pair must fragment a π^- meson. The $d\bar{d}$ pair after the π^+ and π^- emissions remains in the flavor-singlet state, and then repeats meson emissions. Applying Fig. 4 to generate the jet process, we write the resultant gluon fragmentation functions $D_g^{Lm}(z)$ as a combination of the fragmentation functions $D_q^m(z)$ from the quark and $D_{\bar{q}}^m(z)$ from the anti-quark,

$$D_g^{Lm}(z) = \sum_q \frac{1}{3} \int_0^1 P_{g \rightarrow q\bar{q}}(x) \left[D_q^m\left(\frac{z}{x}\right) \frac{1}{x} + D_{\bar{q}}^m\left(\frac{z}{1-x}\right) \frac{1}{1-x} \right] dx, \quad (4)$$

for $z/x \leq 1$ in $D_q^m(z/x)$ and $z/(1-x) \leq 1$ in $D_{\bar{q}}^m(z/(1-x))$. The gluon momentum is distributed between the quark q with the momentum fraction x and the anti-quark \bar{q} with $1-x$ according to the normalized splitting function $P_{g \rightarrow q\bar{q}}$. The average over the three

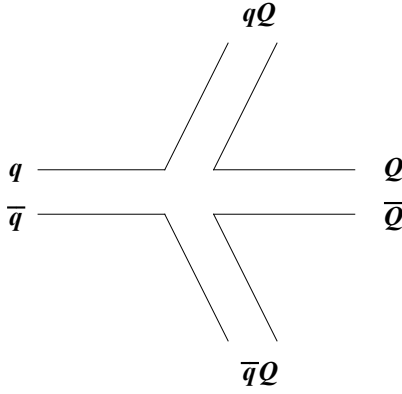


FIG. 4: Gluon elementary fragmentation function in the Lund model.

fictitious quark flavors $q = u, d$, and s has been made explicit. Because D_q^m is defined for an initial quark q with 100% momentum to fragment mesons, its argument should be rescaled, leading to $D_q^m(z/x)/x$ and $D_{\bar{q}}^m(z/(1-x))/(1-x)$ in Eq. (4). This simplest version of our proposal is consistent with the formulation of the gluon fragmentation functions in the Lund model [14].

The choice of the normalized splitting function $P_{g \rightarrow q\bar{q}}$ is arbitrary. Fortunately, we have confirmed that our results are insensitive to the choices of $P_{g \rightarrow q\bar{q}}$, especially after QCD evolution effects are taken into account. Therefore, we simply assume that it is proportional to the Dokshitzer-Gribov-Lipatov-Altarelli-Parisi (DGLAP) kernel [39]

$$P_{g \rightarrow q\bar{q}}(x) = \frac{1}{2}(1 - 2x + 2x^2), \quad (5)$$

for $0 < x < 1$. Our gluon fragmentation functions are also insensitive to the variation of the fictitious quark masses in the involved $d_q^m(z)$ and $d_{\bar{q}}^m$, which are then set to zero for convenience. The values of $g_{\pi qQ}$ and g_{KqQ} are the same as in the previous section. The z dependence of $zD_g^{Lm}(z)$ for a gluon fragmenting into pions and kaons at a model scale are presented in Fig. 5. The features that the probabilities for a gluon to fragment into mesons of different charges are identical, and that the gluon fragmentation functions for kaons are smaller than for pions are expected. We explain why all the gluon fragmentation functions decrease with z by taking the fragmentation into the π^+ meson as an example: the major contributions of $D_{u,\bar{d}}^{\pi^+}$ arise from the high z region, which is suppressed by the phase space $x \geq z$ in Eq. (4), and the contributions of the other quark fragmentation functions are small in the high z region. It should be pointed out that $zD_g^{Lm}(z)$ vanishes as $z \rightarrow 0$ actually,

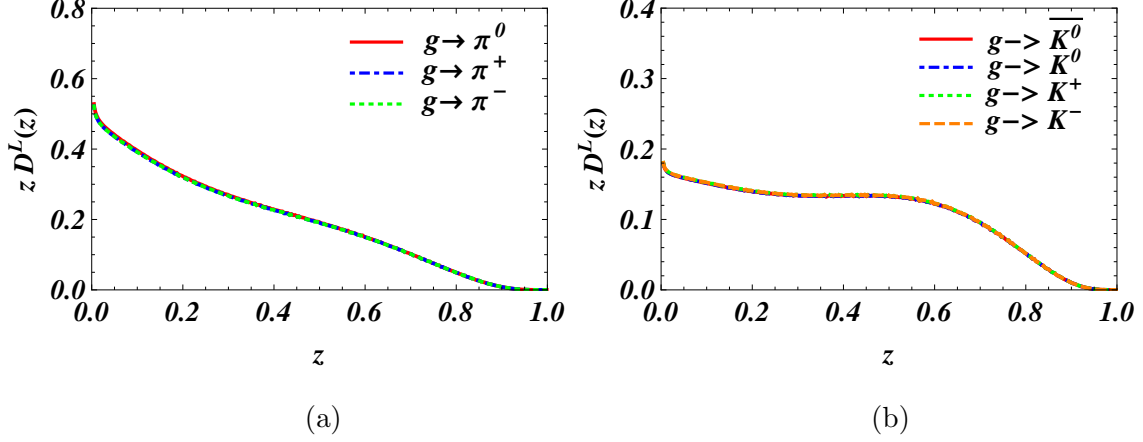


FIG. 5: z dependence of (a) $zD_g^{L\pi}(z)$ and (b) $zD_g^{LK}(z)$ at a model scale.

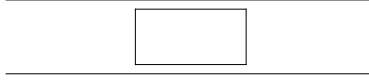


FIG. 6: Color lines for quark annihilation.

though it is hard to see this fact in Fig. 5.

A refined version of our proposal starts with the construction of the elementary gluon fragmentation function $d_g^m(z)$, which describes the probability of a gluon to emit a specific meson m with a momentum fraction z in one step, from the elementary quark fragmentation functions $d_q^m(z)$:

$$d_g^m(z) = \sum_q \frac{1}{3} \int_0^1 P_{g \rightarrow q\bar{q}}(x) \left[d_q^m\left(\frac{z}{x}\right) \frac{1}{x} + d_{\bar{q}}^m\left(\frac{z}{1-x}\right) \frac{1}{1-x} \right] dx, \quad (6)$$

for $z/x \leq 1$ in $d_q^m(z/x)$ and $z/(1-x) \leq 1$ in $d_{\bar{q}}^m(z/(1-x))$. The essential difference of the above construction from the Lund model is that each meson emission by a gluon has no correlation with the previous one: once the quark annihilation mechanism depicted in Fig. 6 is combined with Fig. 4, the quark flavor at each emission is arbitrary (it could be u , d , or s). Namely, the specific flavor of the fictitious $q\bar{q}$ pair is irrelevant, and the color lines mainly provide color sources of meson emissions.

The z dependence of $z d_g^m(z)$ for the one-step fragmentation of a gluon into pions and kaons is displayed in Fig. 7. Similarly, the probabilities for fragmenting into mesons of

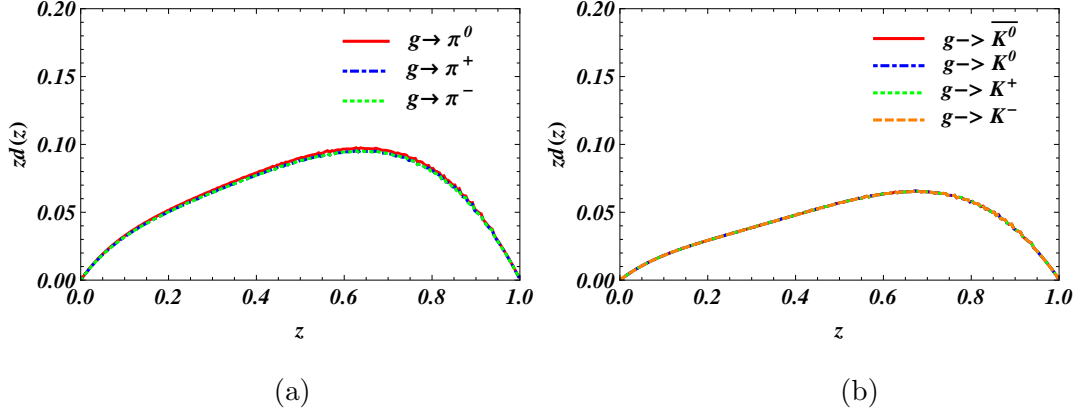


FIG. 7: z dependence of (a) $z d_g^\pi(z)$ and (b) $z d_g^K(z)$.

different charges by a gluon are identical as expected, and the elementary fragmentation functions for kaons are smaller than for pions. The comparison between the behaviors of the gluon and quark elementary fragmentation functions is also similar to the comparison between the gluon and quark fragmentation functions in the Lund model. In the present case the quark elementary fragmentation functions $z d_q^m(z)$ vanish quickly at low z as indicated in Fig. 2, such that $z d_g^m(z)$ also vanish at low z , and have peaks at high z .

Since gluons before and after meson emissions are represented by the pair of color lines without referring to specific quark flavors in the above construct (the memory of specific quark flavors has been washed out by the introduction of the quark annihilation mechanism), the gluon fragmentation function $D_g^m(z)$ satisfies the integral equation

$$D_g^m(z) = \hat{d}_g^m(z) + \sum_{m'} \int_z^1 \frac{dy}{y} \hat{d}_g^{m'}(1-y) D_g^m\left(\frac{z}{y}\right). \quad (7)$$

Note that $d_g^m(z)$ has been normalized into $\hat{d}_g^m(z)$ in order to have a probability meaning, and $\hat{d}_g^{m'}(1-y)$ is interpreted as the probability $\hat{d}_g^{m'}(y)$. The solutions of $z D_g^m(z)$ to Eq. (7) at a model scale are collected in Fig. 8. Compared to the results from the Lund model in Fig. 5, the most significant difference appears in the region of $z < 0.2$, where $z D_g^m(z)$ grow more slowly as z decreases, and descend to zero as $z \rightarrow 0$ more quickly than $z D_g^{Lm}(z)$ do. This difference is attributed to the flavor blindness of the color lines, which renders meson emissions easier and shifts the peaks of the gluon fragmentation functions to a bit higher z .

The gluonic dynamics is more complicated than discussed above definitely. For instance, the fictitious quark pair can split into two or more fictitious quark pairs at any stage of meson emissions. To test the impact of this multi-dipole mechanism, we consider a more

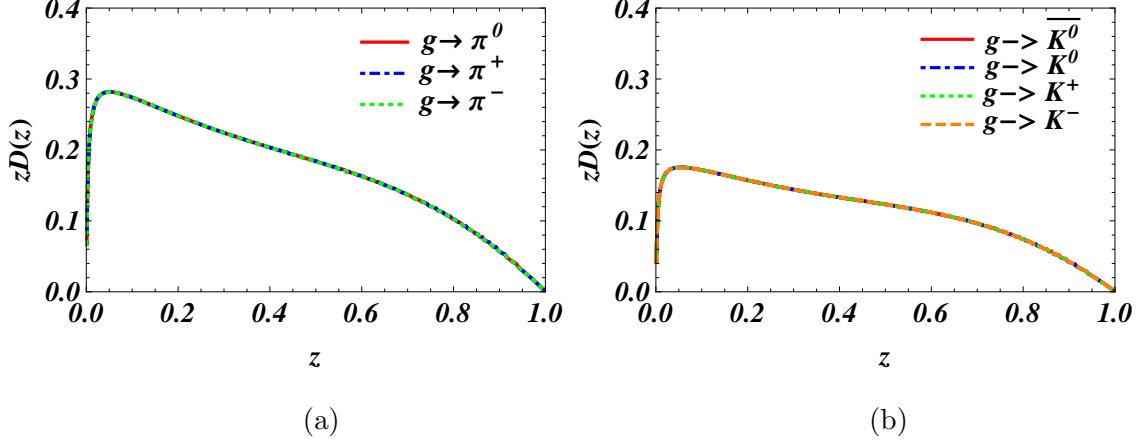


FIG. 8: z dependence of (a) $zD_g^\pi(z)$ and (b) $zD_g^K(z)$ at a model scale.

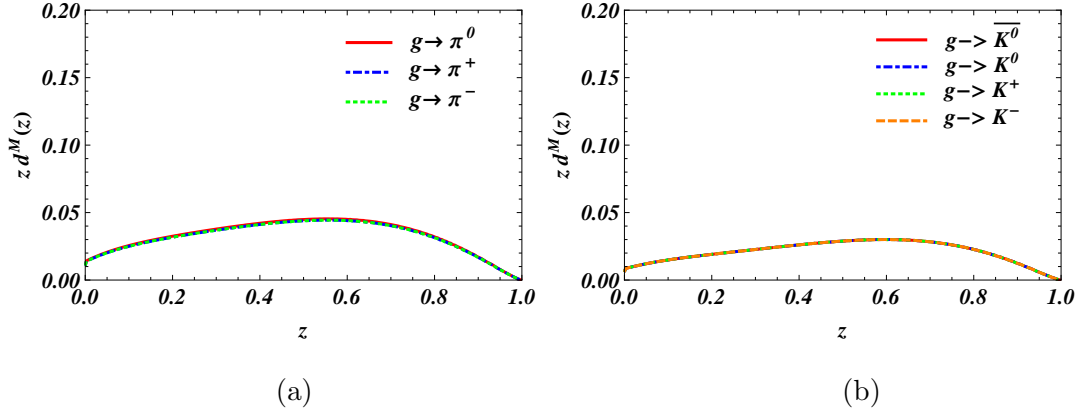


FIG. 9: z dependence of (a) $zd_g^{M\pi}(z)$ and (b) $zd_g^{MK}(z)$.

complicated elementary gluon fragmentation function $d_g^{Mm}(z)$ in terms of $d_g^m(z)$ in Eq. (6):

$$d_g^{Mm}(z) = \int_0^1 P_{g \rightarrow gg}(x) \left[d_g^m\left(\frac{z}{x}\right) \frac{1}{x} + d_g^m\left(\frac{z}{1-x}\right) \frac{1}{1-x} \right] dx, \quad (8)$$

for $z/x \leq 1$ in $d_g^m(z/x)$ and $z(1-x) \leq 1$ in $d_g^m(z/(1-x))$. As a test, the splitting function $P_{g \rightarrow gg}(x)$ is simply chosen to be proportional to the DGLAP kernel

$$P_{g \rightarrow gg}(x) = 6 \left[\frac{1-x}{x} + x(1-x) + \frac{x}{1-x} \right], \quad (9)$$

for $0 < x < 1$. The z dependence of $zd_g^{Mm}(z)$ in Fig. 9 is basically similar to that of $zd_g^m(z)$ in Fig. 7, but more flat. The flatness of $zd_g^{Mm}(z)$ makes the curves of $zD_g^{Mm}(z)$ in Fig. 10 more smooth in the low z region, compared to the curves of $zD_g^m(z)$ in Fig. 8.

A remark is in order. To keep the fictitious quark pair in the flavor-singlet state, the anti-quark must emit a π^- meson, as the quark emits a π^+ meson. One may wonder about

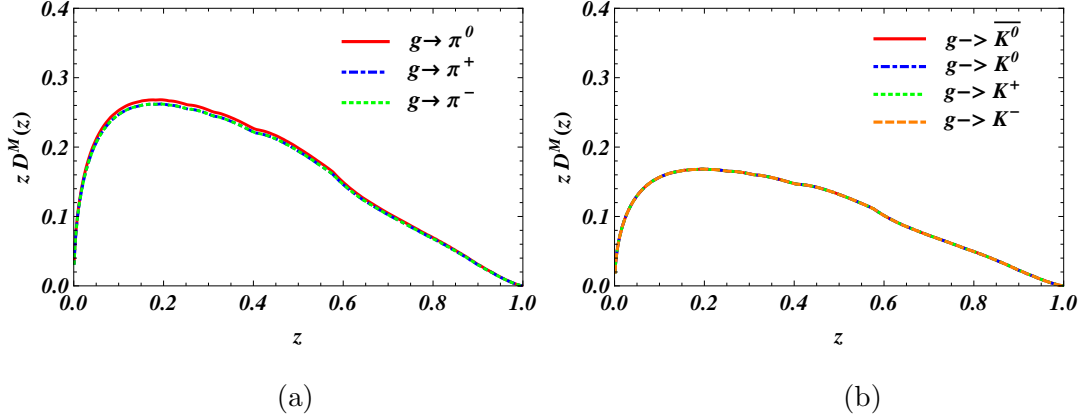


FIG. 10: z dependence of (a) $zD_g^{M\pi}(z)$ and (b) $zD_g^{MK}(z)$ at a model scale.

the channel with only one of the quarks emitting a π^0 meson, which does not defy the flavor-singlet requirement. This π^0 emission seems to enhance the neutral pion production over the charged ones. In fact, this $g \rightarrow g\pi^0$ process should be regarded as the splitting of the quark pair into two quark pairs, whose contribution has been taken into account in the more complicated gluon fragmentation function $D_g^{Mm}(z)$. Hence, the probabilities for a gluon to fragment into charged and neutral pions will be always equal in our approach.

IV. COMPARISON WITH DATA

We have established the gluon fragmentation functions in the NJL model at a model scale, at which the momentum sum rule of those from the scheme consistent with the Lund model gives 1.0072, the sum rule of those including the quark annihilation mechanism gives 0.9612, and the sum rule of those including the multi-dipole contribution gives 0.9045. All of them are close to unity, implying that our numerical analysis is reliable. The plots presented in the previous section show that the gluon fragmentation functions for the charged and neutral pions are the same and those for the four types of kaons are the same too, so we will investigate only the cases of π^+ and K^+ productions here.

We examine the behaviors of the quark and gluon fragmentation functions in different schemes under the LO and NLO QCD evolutions from the model scale $Q_0^2 = 0.15 \text{ GeV}^2$ and $Q_0^2 = 0.17 \text{ GeV}^2$, respectively, to higher scales. The model scales, being free parameters, are chosen to attempt a reasonable fit of the predicted cross section to the SLD data at $Q^2 = M_Z^2$. Note that the model scale for the derivation of the quark fragmentation

functions in the NJL model was set to 0.2 GeV^2 in [32]. For the study of the NLO evolution effect, we adopt the code QCDNUM [40]. Since the observations made from the LO and NLO evolutions are similar, we present only the results of the latter, and collect the former ones in the Appendix. It is worth mentioning that the momentum sum rule for a fragmentation function is indeed violated under the QCD evolution, as postulated in the Introduction, if the gluon fragmentation function was assumed to be null at the model scale: we get $\sum_h \int z D_u^h(z) dz = 0.6488$ and $\sum_h \int z D_g^h(z) dz = 0.1929$ at $Q^2 = 4 \text{ GeV}^2$ under the LO evolution in this case. After including the gluon fragmentation functions, the above values are improved into $\sum_h \int z D_u^h(z) dz = 0.9623$ and $\sum_h \int z D_g^h(z) dz = 0.9334$.

The u -quark and gluon fragmentation functions from the three different schemes at $Q^2 = 4 \text{ GeV}^2$ under the NLO QCD evolution are compared in Fig. 11. The four plots indicate that the evolution effect pushes the difference among the three schemes of handling subtle gluonic dynamics to the region of very small $z < 0.05$. We expect that the difference of the quark and gluon fragmentation functions will move into the region of even lower z , as Q^2 increases up to M_Z^2 . This explains why our results are stable with respect to the variation of model parameters and to the choices of the splitting functions. Besides, the similarity of the curves for zD and zD^M hints that the gluon branching effect may not be crucial. Therefore, it suffices to concentrate only on the scheme with the quark annihilation mechanism below in the scope of the present work.

We then compare our results for the π^+ emission at $Q^2 = 4 \text{ GeV}^2$ with the HKNS [26] and DSS [27] parameterizations, whose initial scale was set to $Q^2 = 1 \text{ GeV}^2$, under the NLO QCD evolution in Fig. 20, and for the K^+ emission in Fig. 21. The comparison at the scale $Q^2 = M_Z^2$ for the π^+ and K^+ emissions is made in Figs. 22 and 23, respectively. In the above plots, the label "NJL without g" in the legend refers to the curves with the gluon fragmentation functions set to zero at the model scale, and the label "NJL with g" refers to the curves including the contribution of the gluon fragmentation functions. Note that the HKNS and DSS parameterizations, extracted from different sets of data, may differ quite a bit in some channels, especially in the low z region. Hence, the comparison just means to give a rough idea on the behaviors of these fragmentation functions obtained in the literature. These figures exhibit obvious difference between the curves labeled by "NJL with g" and by "NJL without g" at $Q^2 = 4 \text{ GeV}^2$ and $Q^2 = M_Z^2$, implying the importance of the gluon fragmentation functions. At both energy scales, the curves for all the π^+ meson

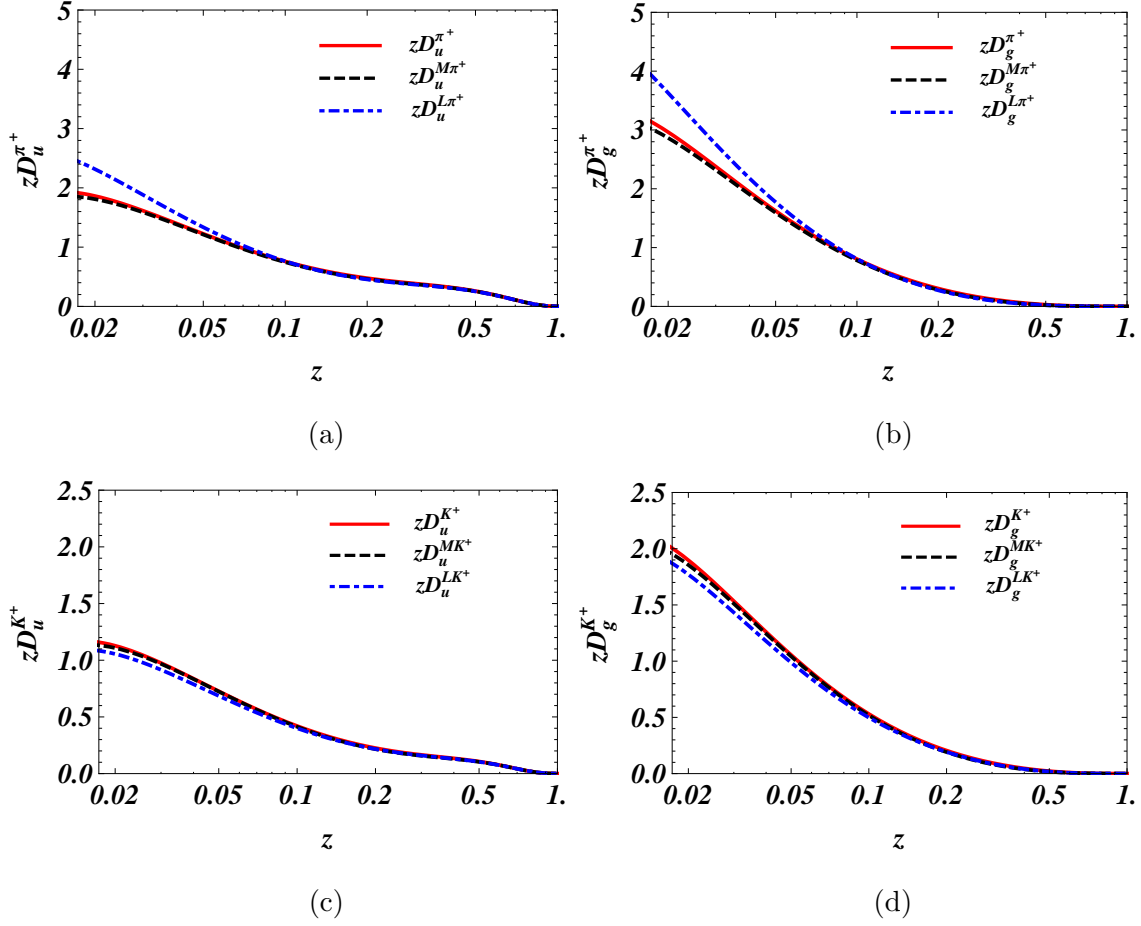


FIG. 11: z dependence of (a) $zD_u(z)$, $zD_u^M(z)$, and $zD_u^L(z)$, and (b) $zD_g(z)$, $zD_g^M(z)$, and $zD_g^L(z)$ for the π^+ meson emission at the scale $Q^2 = 4 \text{ GeV}^2$ under the NLO evolution. (c) and (d) are for the K^+ meson emission.

channels labeled by "NJL with g" are closer to the HKNS or DSS ones than those labeled by "NJL without g" in the almost entire region of z . For the K^+ meson channels at both $Q^2 = 4 \text{ GeV}^2$ and $Q^2 = M_Z^2$, it is hard to tell which curves, "NJL with g" or "NJL without g", are closer to the HKNS and DSS ones. However, the "NJL with g" ("NJL without g") curves seem to be closer to the HKNS (DSS) ones at $Q^2 = M_Z^2$. It is a general trend that all the curves are more distinct in the low z region.

Next we predict the $e^+ + e^- \rightarrow h + X$ differential cross section [42]

$$F^h(z, Q^2) \equiv \frac{1}{\sigma_{tot}} \frac{d\sigma(e^+ + e^- \rightarrow h + X)}{dz}, \quad (10)$$

using the quark and gluon fragmentation functions from the previous section, where $z = 2E_h/\sqrt{s} = 2E_h/Q$ is the energy fraction, with E_h being the energy carried by the hadron h ,

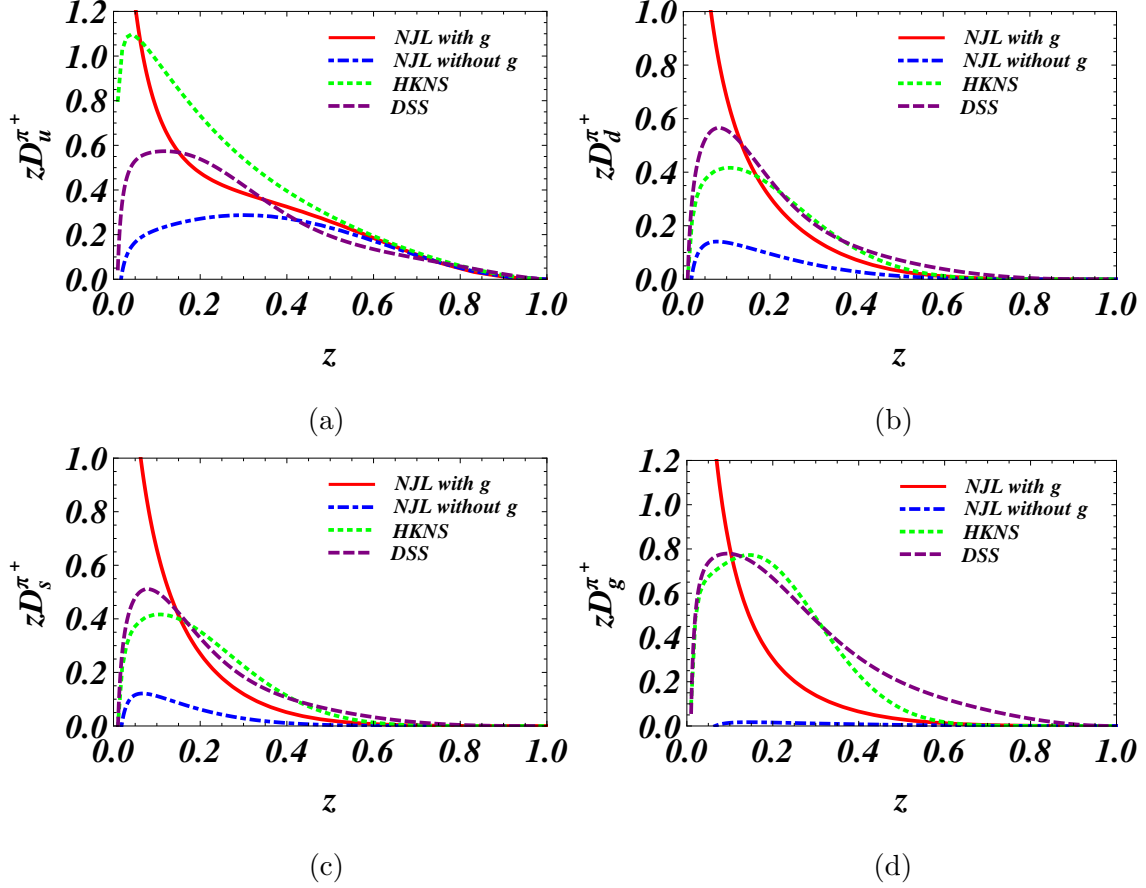


FIG. 12: Comparison of (a) $zD_u^{\pi^+}(z)$, (b) $zD_d^{\pi^+}(z)$, (c) $zD_s^{\pi^+}(z)$, and (d) $zD_g^{\pi^+}(z)$ with the HKNS and DSS parameterizations at the scale $Q^2 = 4 \text{ GeV}^2$ under the NLO evolution.

\sqrt{s} being the center of mass energy, and Q being the invariant mass of the virtual photon or Z boson. According to the factorization theorem, Eq. (10) can be written as a convolution of two subprocesses [41]: the hard scattering part $e^+ + e^- \rightarrow \gamma(Z) \rightarrow q + \bar{q}$ at LO or $e^+ + e^- \rightarrow \gamma(Z) \rightarrow q + \bar{q} + g$ at NLO, which is calculable in perturbative QCD, and the hadronic part $q + \bar{q}(q + \bar{q} + g) \rightarrow h + X$, which involves nonperturbative dynamics. The latter is described by the fragmentation functions for the hadron h emitted by the partons q , \bar{q} , or g . We have the factorization formula [42]

$$F^h(z, Q^2) = \sum_i C_i(z, \alpha_s) \otimes D_i^h(z, Q^2), \quad (11)$$

where the subscript $i = u, d, s, \dots, g$ denotes flavors of partons, the coefficient functions $C_i(z, \alpha_s)$ have been computed up to NLO in the modified minimal subtraction scheme [43], and $D_i^h(z, Q^2)$ denotes the parton i fragmentation function for the hadron h . The convolution

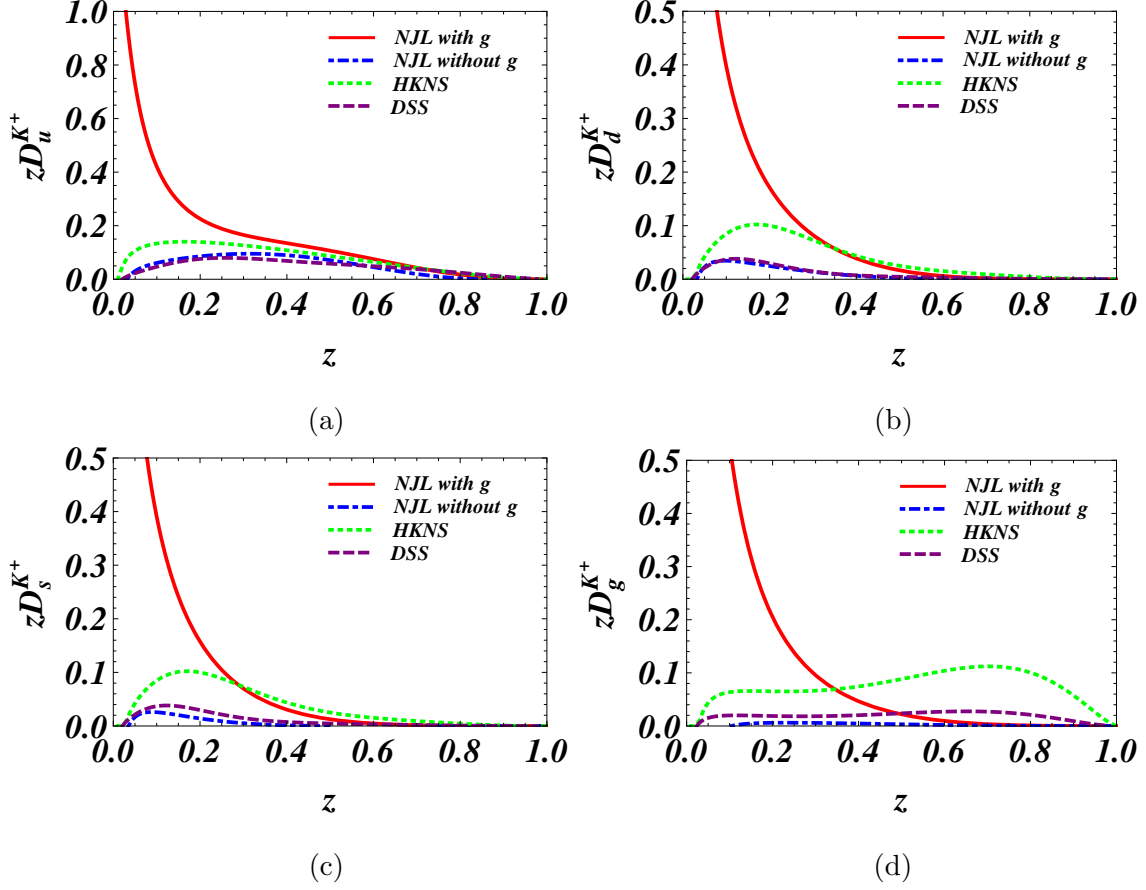


FIG. 13: Same as Fig. 12, but for the K^+ meson emission.

\otimes is defined by

$$f(z) \otimes g(z) = \int_z^1 \frac{dy}{y} f(y) g\left(\frac{z}{y}\right). \quad (12)$$

Our predictions for $F^h(z, Q^2)$ in Eq. (11), $h = \pi$ and K , are compared to the SLD data [21] at the scale $Q^2 = M_Z^2$ under the LO and NLO evolutions in Fig. 16. It is observed in all the plots that the curves labeled by "NJL without g" are significantly lower than the SLD data for $z < 0.4$, and higher than the SLD data for $z > 0.4$ in the pion channel. The inclusion of the gluon fragmentation functions, correcting the above tendency, improves the overall consistency with the data. This improvement highlights the phenomenological impact of the gluon fragmentation functions, and their importance for accommodating the data. In particular, the "NJL with g" predictions agree well with the SLD data in the pion channel, after the NLO evolution is implemented. It is roughly the case in the kaon channel, but with the "NJL with g" predictions overshooting the data in the small $z < 0.2$ region. However, the curves labeled by "NJL with g" from the NLO evolution are very close to the

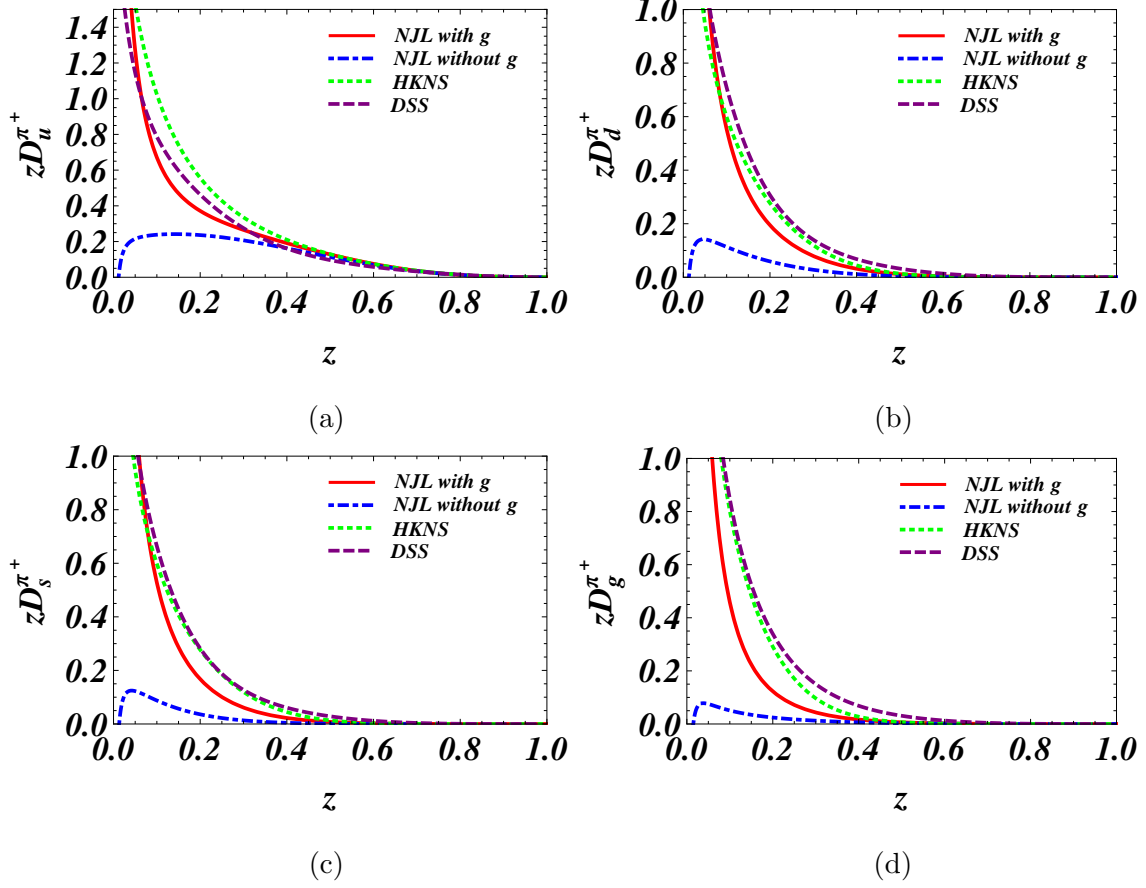


FIG. 14: Comparison of (a) $zD^{\pi^+}_u(z)$, (b) $zD^{\pi^+}_d(z)$, (c) $zD^{\pi^+}_s(z)$, and (d) $zD^{\pi^+}_g(z)$ with the HKNS and DSS parameterizations at the scale $Q^2 = M_Z^2$ under the NLO evolution.

HKNS and DSS parameterizations in both the pion and kaon channels. The agreement of the predictions with the data supports our proposal to treat a gluon as a pair of color lines in the NJL model.

At last, we check the sensitivity of our results to the variation of some model parameters. Figure 17 shows the u -quark and gluon fragmentation functions for the π^+ meson under the NLO evolution from three different initial model scales $Q_0^2 = 0.15, 0.17$, and 0.20 GeV^2 to $Q^2 = 4 \text{ GeV}^2$. It is found that the quark fragmentation function is more sensitive to the variation of the model scale than the gluon fragmentation function. It hints that the $e^+ + e^- \rightarrow h + X$ differential cross section at high z , dominated by the contribution from the quark fragmentation functions, depends more strongly on the model scale. We have taken into account this property, as determining the model scales via reasonable fits of our predictions to the SLD data. The sensitivity of the gluon fragmentation functions for the

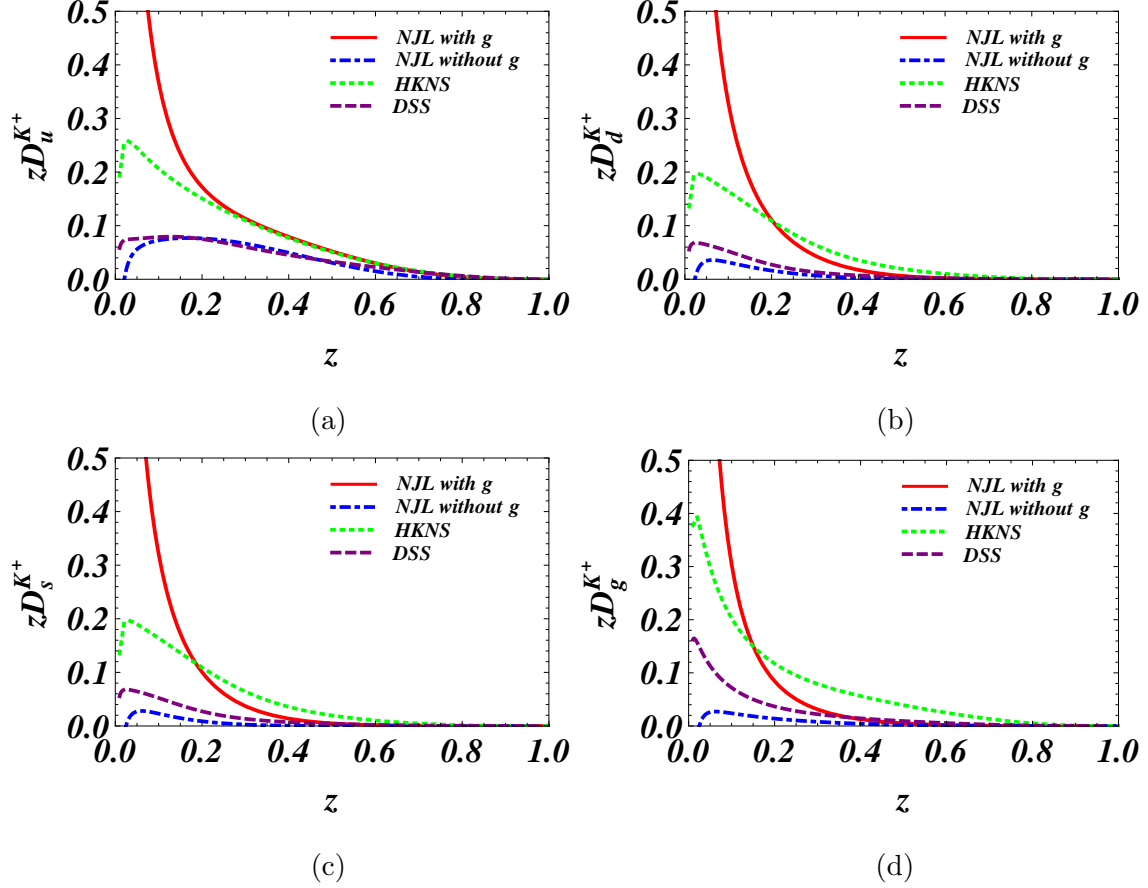


FIG. 15: Same as Fig. 14, but for the K^+ meson emission.

π^+ and K^+ mesons at the model scale to the fictitious quark mass is examined in Fig. 18. The difference among the three sets of curves for $M_1 = M_2 = 0.0, 0.2$, and 0.4 GeV in the region of finite z turns out to be easily smeared by the QCD evolution effect. It explains why we have adopted the input $M_1 = M_2 = 0.0$ for convenience in this work.

V. CONCLUSION

In this paper we have derived the gluon fragmentation functions in the NJL model by treating a gluon as a pair of color lines formed by fictitious quark and anti-quark under the requirement that they remain in the flavor-singlet state after simultaneous meson emissions. The idea originates from the color dipole model, in which the same treatment turns parton emissions into emissions of color dipoles. The gluon fragmentation functions were then formulated in terms of the quark fragmentation functions accordingly. The simplest version

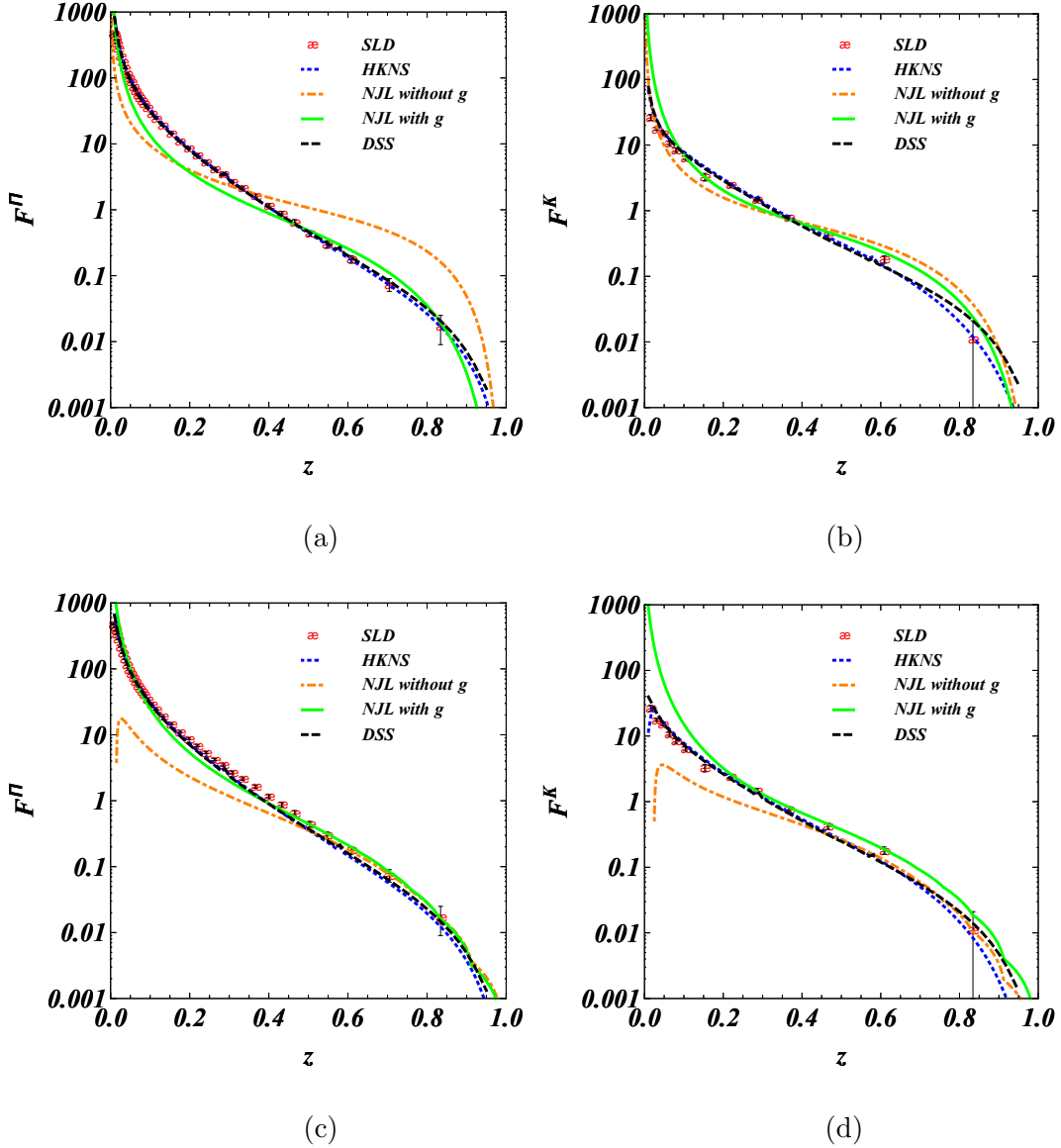


FIG. 16: Our predictions for $F^h(z, Q^2)$ compared with the SLD data, and the HKNS and DSS parameterizations at the scale $Q^2 = M_Z^2$ for (a) $h = \pi$ and (b) $h = K$ under the LO evolution. Same for (c) and (d) under the NLO evolution.

of our proposal is consistent with that in the Lund model [14], as a combination of the quark and anti-quark fragmentation functions. A refined version is to include the quark annihilation mechanism, such that the specific flavor of the fictitious quarks is irrelevant, and the color lines just serve as color sources of meson emissions. The corresponding gluon elementary fragmentation functions constructed from the quark and anti-quark elementary fragmentation functions lead to the integral equation, as a consequence of the iterations of

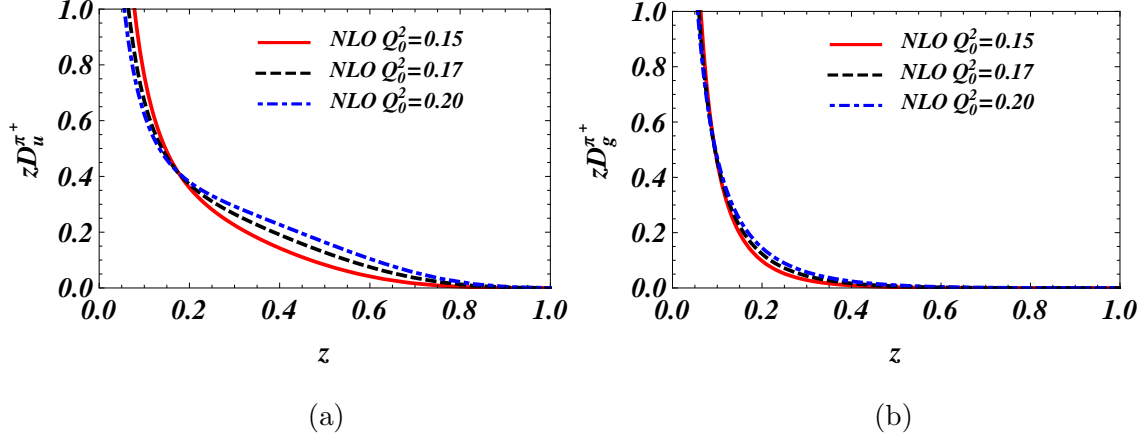


FIG. 17: z dependence of (a) $zD_u^{\pi^+}(z)$ and (b) $zD_g^{\pi^+}(z)$ at the scale $Q^2 = 4 \text{ GeV}^2$ for three different values of Q_0^2 (in units of GeV^2).

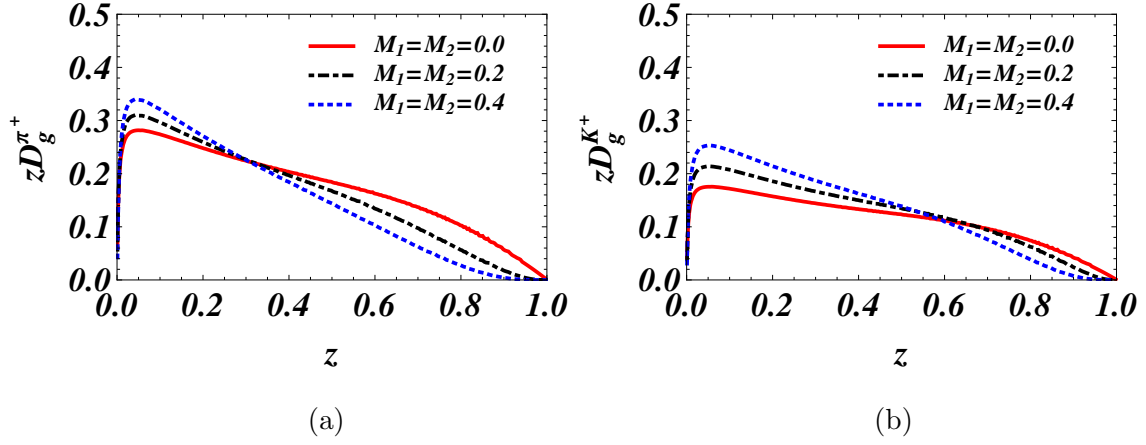


FIG. 18: z dependence of (a) $zD_g^{\pi^+}(z)$ and (b) $zD_g^{K^+}(z)$ at the model scale for three different values of $M_1 = M_2$ (in units of GeV).

the elementary fragmentation into a jet process. The gluon branching effect, i.e., the multi-dipole contribution to the gluon fragmentation was also discussed in the same framework, and found to be minor.

The results from the above three different schemes of handling subtle gluonic dynamics were compared at the model scale, and evolved to higher scales. It has been confirmed that the QCD evolution effect pushes the difference among the three schemes to the region of very small z . This explains why our results are stable with respect to the variation of the model parameters and to the choices of the splitting functions. We have demonstrated that the inclusion of the gluon fragmentation functions into the theoretical predictions from only

the quark fragmentation functions greatly improves the agreement with the SLD data for the pion and kaon productions in e^+e^- annihilation at the scale $Q^2 = M_Z^2$. Especially, our predictions for the pion emission from the NLO evolution are well consistent with the SLD data, and with the HKNS and DSS parameterizations. This nontrivial consistency implies that our proposal may have provided a plausible construct for the gluon fragmentation functions, which are supposed to be null in the NJL model.

The framework presented in this paper is ready for a generalization to the quark and gluon fragmentation functions for other pseudoscalar mesons, such as η and η' . Wide applications are expected. The heavy-quark (charm and bottom) fragmentation functions should be included for a complete QCD evolution to Q^2 as high as M_Z^2 , which have been taken into account in the HKNS and DSS parameterizations. How to establish the heavy-quark fragmentation functions in an effective model is another challenging and important mission. We will address these subjects in future works.

Appendix A: RESULTS UNDER LO EVOLUTION

We collect some results from the LO evolution in this appendix. Figure 19 displays the similarity of the quark and gluon fragmentation functions from the the three different schemes, namely, the scheme consistent with the Lund model, the scheme including the quark annihilation mechanism, and the scheme including the multi-dipole contribution, under the LO evolution. This similarity supports the consideration of only the scheme with the quark annihilation mechanism.

Our results for the quark and gluon fragmentation functions are compared with the HKNS and DSS parameterizations at the scales $Q^2 = 4 \text{ GeV}^2$ and $Q^2 = M_Z^2$ under the LO evolution in Figs. 20-23. Similar to the observation drawn from the NLO evolution, the obvious difference between the curves labeled by "NJL with g" and by "NJL without g" indicates the importance of the gluon fragmentation functions. For any quark or gluon to the π^+ meson channels, the "NJL with g" results agree better with the HKNS and DSS ones than the "NJL without g" results do at $Q^2 = 4 \text{ GeV}^2$ and $Q^2 = M_Z^2$ in the almost entire region of z . For the K^+ meson channels, it is hard to tell which curves, "NJL with g" or "NJL without g" are closer to the HKNS and DSS ones. Again, all the curves are more distinct in the low z region.

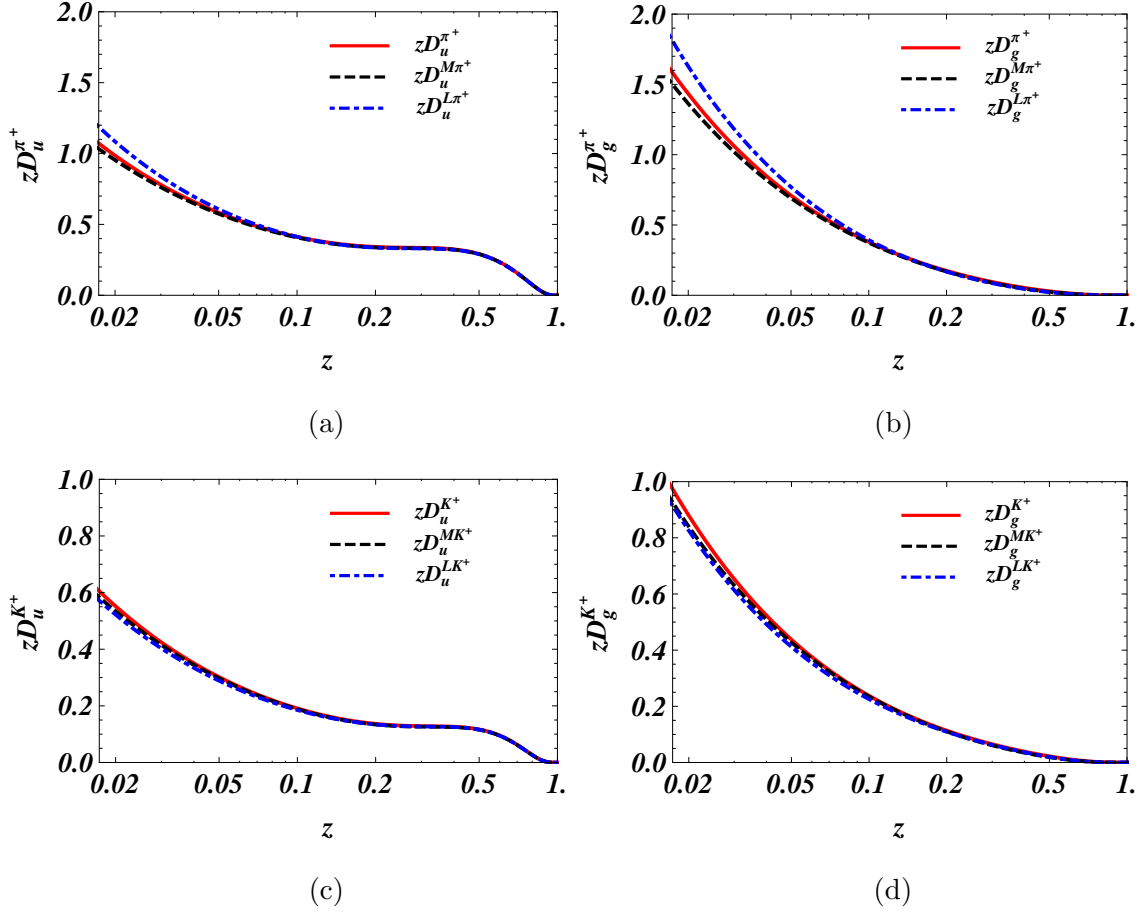


FIG. 19: z dependence of (a) $zD_u(z)$, $zD_u^M(z)$, and $zD_u^L(z)$, and (b) $zD_g(z)$, $zD_g^M(z)$, and $zD_g^L(z)$ for the π^+ meson emission at the scale $Q^2 = 4 \text{ GeV}^2$. (c) and (d) are for the K^+ meson emission.

Acknowledgments

This work was supported in part by the Ministry of Science and Technology of R.O.C.. Hsiang-nan Li is supported by Grant No. MOST-104-2112-M-001-037-MY3 from Ministry of Science and Technology (MOST) of Taiwan. Dong-Jing Yang is supported by MOST of Taiwan (Grant No. MOST-102-2112-M-033-005-MY3).

-
- [1] J. C. Collins, Nucl. Phys. **B396**, 161 (1993).
 - [2] P. J. Mulders and R.D. Tangerman, Nucl. Phys. **B461**, 197 (1996).
 - [3] D. Boer and P. J. Mulders, Phys. Rev. D **57**, 5780 (1998).

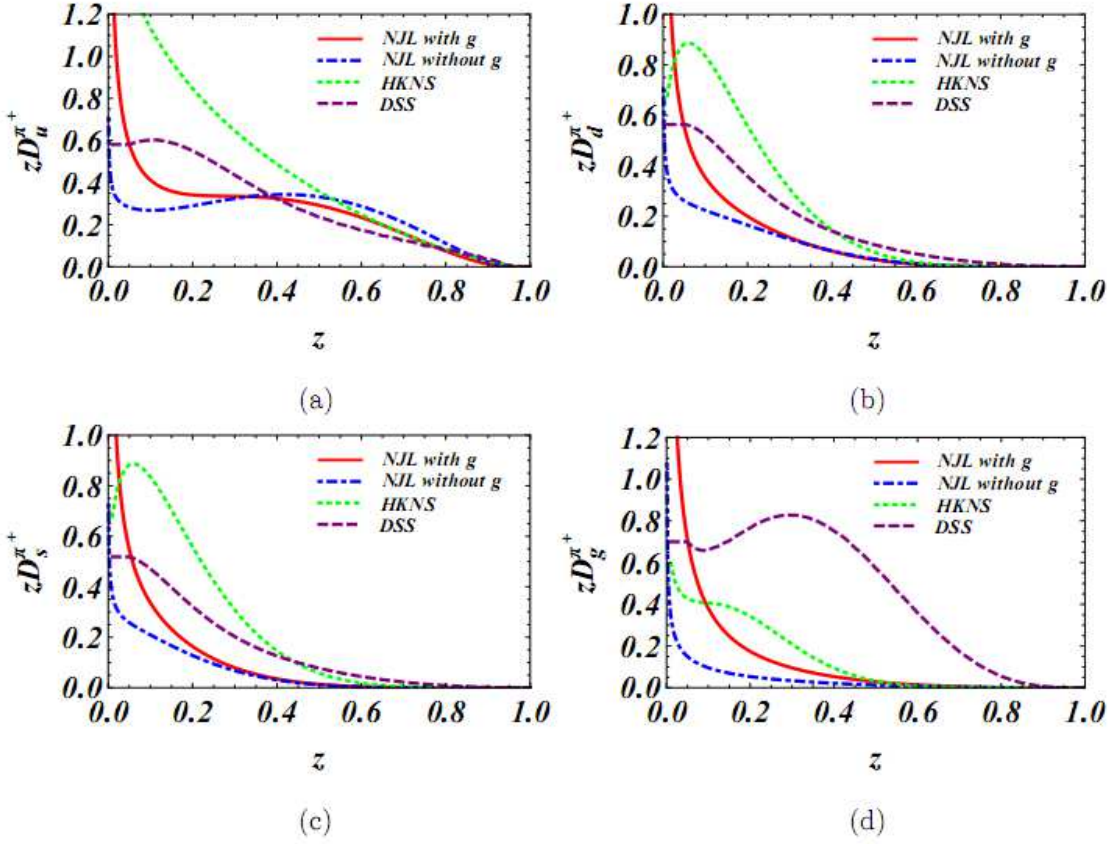


FIG. 20: Comparison of (a) $zD_u^{\pi^+}(z)$, (b) $zD_d^{\pi^+}(z)$, (c) $zD_s^{\pi^+}(z)$, and (d) $zD_g^{\pi^+}(z)$ with the HKNS and DSS parameterizations at the scale $Q^2 = 4 \text{ GeV}^2$ under the LO evolution.

- [4] M. Anselmino, M. Boglione, and F. Murgia, Phys. Lett. B **362**, 164 (1995).
- [5] M. Anselmino, M. Boglione, U. D'Alesio, E. Leader, S. Melis, F. Murgia, and A. Prokudin, arXiv:0907.3999 [hep-ph].
- [6] E. Christova and E. Leader, Eur. Phys. J. C **51**, 825 (2007).
- [7] M. Anselmino, M. Boglione, U. D'Alesio, A. Kotzinian, F. Murgia, A. Prokudin, and C. Türk, Phys. Rev. D **75**, 054032 (2007).
- [8] A. Bacchetta, M. Diehl, K. Goeke, A. Metz, P. J. Mulders, and M. Schlegel, JHEP **02**, 093 (2007).
- [9] A.V. Efremov, K. Goeke, and P. Schweitzer, Phys. Rev. D **73**, 094025 (2006).
- [10] J. C. Collins, A.V. Efremov, K. Goeke, S. Menzel, A. Metz, and P. Schweitzer, Phys. Rev. D **73**, 014021 (2006).
- [11] X. d. Ji, J. p. Ma, and F. Yuan, Phys. Rev. D **71**, 034005 (2005).

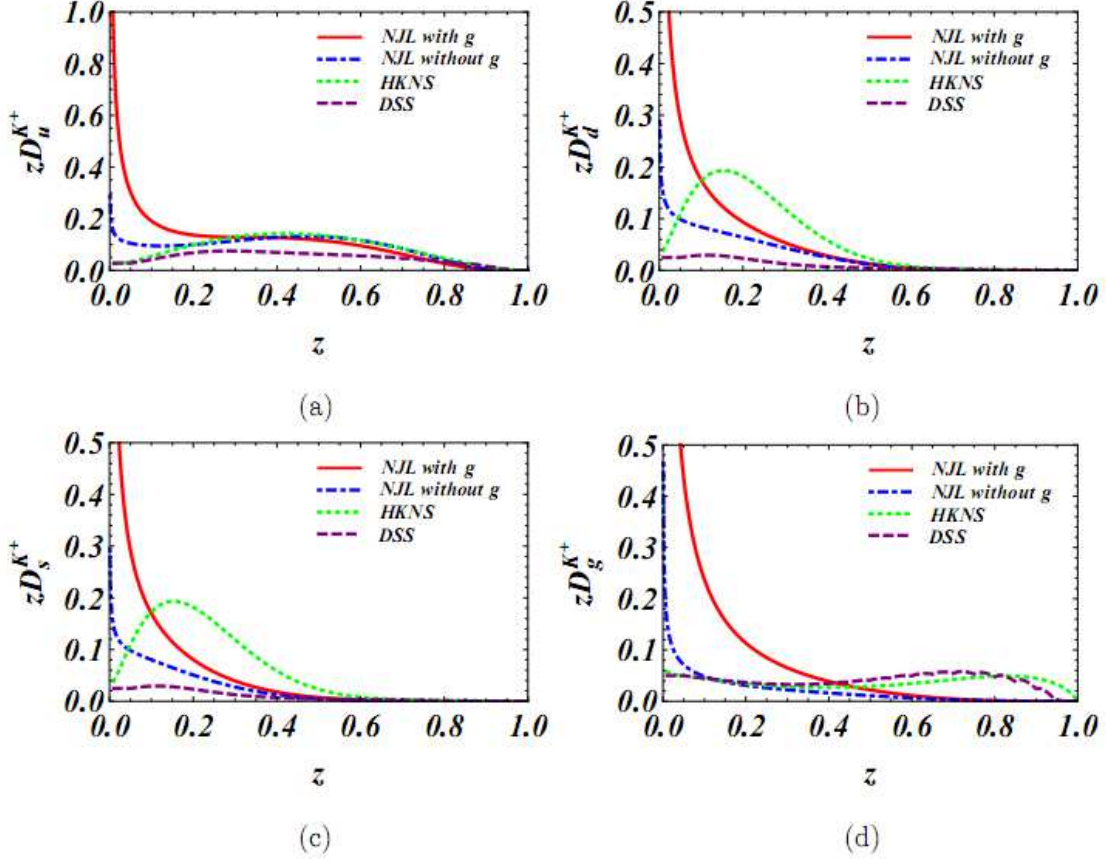


FIG. 21: Same as Fig. 20, but for the K^+ meson emission.

- [12] H. H. Matevosyan, A. W. Thomas, and W. Bentz, Phys. Rev. D **83**, 114010 (2011).
- [13] D. J. Yang, F. J. Jiang, C.W. Kao, and S. I. Nam, Phys. Rev. D **87**, 094007 (2013).
- [14] B. Andersson, G. Gustafson, G. Ingelman, and T. Sjöstrand, Phys. Rept. **97**, 31 (1983).
- [15] R. Brandelik et al. (TASSO Collaboration), Phys. Lett. B **94**, 444 (1980).
- [16] M. Althoff et al. (TASSO Collaboration), Z. Phys. C **17**, 5 (1983).
- [17] W. Braunschweig et al. (TASSO Collaboration), Z. Phys. C **42**, 189 (1989).
- [18] H. Aihara et al. (TPC Collaboration), Phys. Rev. Lett. **52**, 577 (1984); **61**, 1263 (1988).
- [19] M. Derrick et al. (HRS Collaboration), Phys. Rev. D **35**, 2639 (1987).
- [20] R. Itoh et al. (TOPAZ Collaboration), Phys. Lett. B **345**, 335 (1995).
- [21] K. Abe et al. (SLD Collaboration), Phys. Rev. **D69**, 072003 (2004).
- [22] D. Buskulic et al. (ALEPH Collaboration), Z. Phys. C **66**, 355 (1995); R. Barate et al., Phys. Rep. **294**, 1 (1998).
- [23] R. Akers et al. (OPAL Collaboration), Z. Phys. C **63**, 181 (1994).

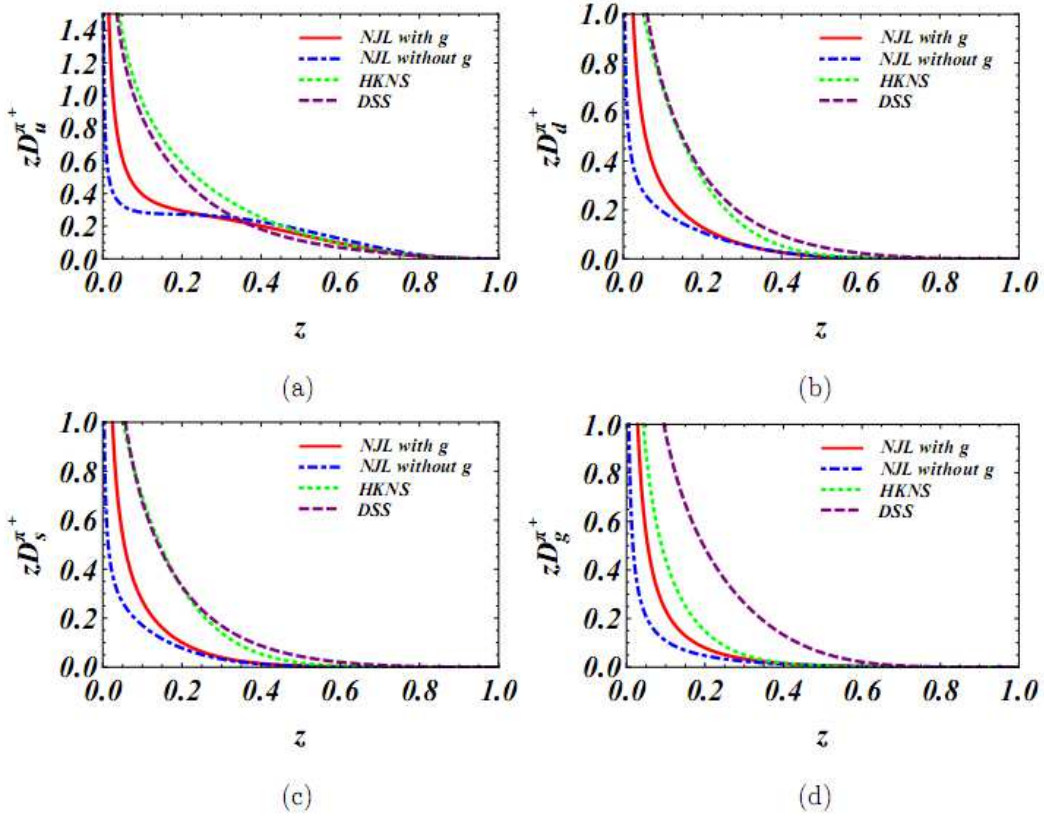


FIG. 22: Comparison of (a) $zD_u^{\pi^+}(z)$, (b) $zD_d^{\pi^+}(z)$, (c) $zD_s^{\pi^+}(z)$, and (d) $zD_g^{\pi^+}(z)$ with the HKNS and DSS parameterizations at the scale $Q^2 = M_Z^2$ under the LO evolution.

- [24] P. Abreu et al. (DELPHI Collaboration), Eur. Phys. J. **C5**, 585 (1998).
- [25] P. Abreu et al. (DELPHI Collaboration), Nucl. Phys. **B444**, 3 (1995).
- [26] M. Hirai, S. Kumano, T. H. Nagai, and K. Sudoh, Phys. Rev. D **75**, 094009 (2007).
- [27] D. de Florian, R. Sassot, and M. Stratmann, Phys. Rev. D **75**, 114010 (2007).
- [28] Y. Nambu, G. Jona-Lasinio, Phys. Rev. **122**, 345 (1961).
- [29] Y. Nambu, G. Jona-Lasinio, Phys. Rev. **124**, 246 (1961).
- [30] T. Shigetani, K. Suzuki and H. Toki, Phys. Lett. B **308**, 383 (1993).
- [31] R. M. Davidson and E. Ruiz Arriola, Phys. Lett. B **359**, 273 (1995).
- [32] H. H. Matevosyan, A. W. Thomas, and W. Bentz, Phys. Rev. D **83**, 074003 (2011).
- [33] H. H. Matevosyan, W. Bentz, I. C. Cloet, and A. W. Thomas, Phys. Rev. D **85**, 014021 (2012).
- [34] R. D. Field and R. P. Feynman, Nucl. Phys. **B136**, 1 (1978).

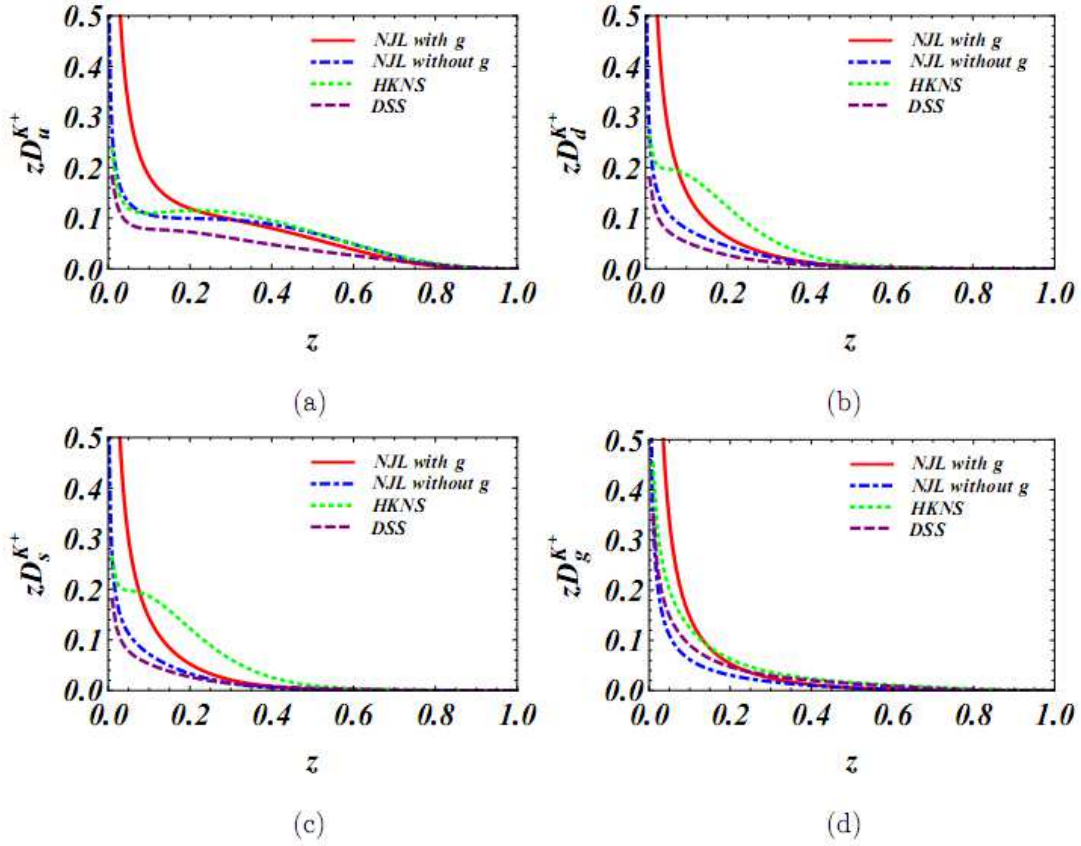


FIG. 23: Same as Fig. 22, but for the K^+ meson emission.

- [35] G. Gustafson, Phys. Lett. B **175**, 453 (1986).
- [36] G. Gustafson and U. Pettersson, Nucl. Phys. **B306**, 746 (1988).
- [37] L. B. Andersson, G. Gustafson, Lönblad, and U. Pettersson, Z. Phys. C **43**, 625 (1989).
- [38] A. H. Mueller and B. Patel, Nucl. Phys. **B425**, 471 (1994).
- [39] V.N. Gribov and L.N. Lipatov, Sov. J. Nucl. Phys. **15**, 428 (1972); G. Altarelli and G. Parisi, Nucl. Phys. **B126**, 298 (1977); Yu.L. Dokshitzer, Sov. Phys. JETP **46**, 641 (1977).
- [40] M. Botje, Comput. Phys. Commun. **182**, 490 (2011).
- [41] F. Halzen and A. D. Martin, *Quarks and Leptons: An Introductory Course in Modern Particle Physics*, John Wiley & Sons (1984).
- [42] R. K. Ellis, W. J. Stirling, and B. R. Webber, *QCD and Collider Physics*, Cambridge University Press (1996).
- [43] S. Kretzer, Phys. Rev. D **62**, 054001 (2000).